Supplementary Material (ESI) for Chemical Communications

Simultaneous detection of enterovirus 71 and coxsackievirus A16 using dual-color upconversion luminescent nanoparticle as labels

1. Reagents and Apparatus

Reagents. Rare-earth oxides used in this work, including yttrium oxide (Y_2O_3), ytterbium oxide (Yb_2O_3), erbium oxide (Er_2O_3) and thulium oxide (Tm_2O_3) were of 99.99% purity. hydrofluoric acid (HF), 25% ammonia ($NH_3 \cdot H_2O$), sodium hydroxide (NaOH), nitric acid (HNO_3), cetyltrimethyl ammonium bromide (CTAB), ethylene diamine tetraacetic acid (EDTA), 1,6-hexylenediamime, anhydrous natrium aceticum (CH_3COONa), iron trichloride ($FeCl_3 \cdot 6H_2O$), 25% glutaraldehyde ($OHC(CH_2)_3CHO$) and tetraethyl orthosilicate (TEOS) were of analytical grade. All the chemicals above were purchased from Sinopharm Chemical Reagent Co., Ltd. (Shanghai, China). 98% 3-aminopropyltrimethoxysilane (APTES) was purchased from Alfa Aesar (U.S.A.). 99% avidin was purchased from Sigma (U.S.A.).

Table 1 Table 1 ssDNA sequences for detection EV71 and CV-A16 were purchased from Sangon Biotechnology Co., Ltd. (Shanghai, China)

	Designation	Sequence (5'-3')	Size(bp)
DNA1	EV-71 probe	TCGATAGTTTCTT-Biotin	13
DNA2	EV-71 capture	Biotin-TCGCACAGCACAGCTGAGACC ACTC	25
DNA3	EV-71 target	AAGAAACTATCGAGAGTGGTCTCAG CTGTGCTGTGCGA	38
DNA4	CV-A16 probe	CCGGTTTGGTTAGCA-Biotin	15
DNA5	CV-A16 capture	Biotin-CAGCCATTGGGAATTTCTTTA GCCGTG	27
DNA6	CV-A16 target	TAACCAAACCGGCACGGCTAAAGA AATTCCCAATGGCTG	39

Apparatus. The size and morphology of nanoparticles were observed on a JEM-2100HR transmission electron microscope (TEM, JEOL Ltd., Japan), using an accelerating voltage of 200 kV. X-ray diffraction (XRD) measurements were performed on a D8-advance (Bruker AXS Ltd., Germany) with graphite-monochromatized Cu Kα radiation (λ=0.15406 nm).The operation voltage and current were kept at 40 kV and 40 mA, respectively. A 2θ range from 10º to 70º was covered in steps of 0.02º with a count time of 2s. UCNPs fluorescence spectra were measured on an F-7000 fluorescence spectrophotometer (Hitachi Co., U.S.A.) attached to an external 980 nm laser (Beijing Hi-Tech Optoelectronic Co., China) instead of the internal excitation source. The maximum power of the laser was 1300 mW. Ultraviolet-visible (UV-vis) absorption spectra were recorded by using a Shimadzu UV-2300 UV-vis spectrophotometer (Shimadzu, Japan). FTIR spectra of the amino-functionalized NPs were conducted with a Nicolet Nexus 470 Fourier transform infrared spectrophotometer (Thermo Electron Co., U.S.A.) by using the KBr method. The suspension of NPs was prepared by using an ultrasonic bath KJ-300 (Wuxi Kejie Electron Instruments Co., Ltd. China).

2. Synthesis and surface modification of $NaYF_4$:Yb, Er/Tm UCNPs

$NaYF_4$:Yb, Er/Tm UCNPs were synthesized based on the hydro-thermal method.[1-2] Briefly, a mixture of 0.18 g of Y_2O_3 (28 %), 0.788 g Yb_2O_3 (70 %) and 0.022 g Er_2O_3 (2 %), was dissolved in nitric acid by heating, and the solvent was evaporated to form the rare-earth nitrate powder and then dissolved in 8 mL demonized water. The transparent EDTA-Ln^{3+} solution was acquired by adding 1.0635g EDTA and adjusting the pH to weak basic conditions (pH 8.0). 3 mL of hydrofluoric acid (HF) was added to 25 mL glycol as the fluorine origin, then 0.4g CTAB was added to increase the amount of the carbon in the reaction system to prevent the nanoparticles from aggregating. Under vigorous stirring, 8 mL of the EDTA-Ln^{3+} solution was dripped, followed by the addition of 3.5 mL of nitric acid. The mixed solution was transferred into a Teflon-lined autoclave and heated to 195 ºC for 18h. After the autoclave was cooled to room temperature naturally, the UCNPs were deposited at the bottom of the vessel, washed with hot water to the beaker, ultrasonic dispersed for 10 min, placed for several minutes then the

supernatant was discarded, repeated three times. The UCNPs were purified by centrifugation, washed with ethanol three times, and dried at 60 °C for 12 h. $NaY_{0.28}F_4$:$Yb_{0.70}$, $Er_{0.02}$ UCNPs were thus formed. In accordance with the above method, the ratio of rare earth doped was changed, $NaY_{0.78}F_4$:$Yb_{0.20}$, $Tm_{0.02}$ UCNPs were thus formed.

Surface modification of $NaYF_4$: Yb, Er/Tm UCNPs was completed by using a typical Stöber-based method.[3] In a 250 mL flask, 20 mg of UCNPs were dispersed in 60 mL of 3-propanol by sonication and agitation for 40 min, then 2.5 mL of ammonia and 20 mL of water were added to the flask, and the mixture was maintained at 35 °C under vigorous stirring. A solution containing 20 mL of 3-propanol and 50 μL of TEOS was added dropwise to the mixture over a period of 1 h, and the reaction was continued for another 3 h. A solution containing 30 mL of 3-propanol and 200 μL of APTES was then added dropwise into the suspension, the reaction was continued for 1 h. When the reaction terminated the product was “aged” for 2 hour at room temperature. Than the precipitates were separated by centrifugation, washed with ethanol three times, and then dried at 60 °C for 12 h to obtain amino-functionalized UCNPs. Amino-modified $NaYF_4$: Yb, Er/Tm UCNPs were thus formed.

3. Preparation of amine-functionalized Fe_3O_4 MNPs

Amine-functionalized Fe_3O_4 MNPs were prepared with one-pot synthesis.[4] In the case of ~25 nm magnetic nanoparticles, a solution of 6.5 g 1,6-hexanediamine, 2.0 g anhydrous sodium acetate and 1.0 g $FeCl_3 \cdot 6H_2O$ as a ferric source in 30 mL glycol was stirred vigorously at 50 °C to give a transparent solution. This solution was then transferred into a Teflonlined autoclave and reacted at 198 °C for 6 h. The magnetite nanoparticles were then rinsed with water and ethanol (2 or 3 times) to effectively remove the solvent and unbound 1,6-hexanediamine, and then dried at 50 °C before characterization and application. During each rinsing step, the nanoparticles were separated from the supernatant by using magnetic force.

4. Preparation of avidin-conjugated nanoparticles

Typically, 10 mg of amino-modified NPs was dispersed in 5 mL of 10 mmol/L

phosphate buffer solution (PBS) of pH 7.4 by ultrasonication for 15 min, and then 1.25 mL of 25% glutaraldehyde was added into the mixture. The mixture was shaken slowly on a shaking table at room temperature for 2 h, and the UCNPs were separated by centrifugation and magnetic nanoparticles were magnetic separated then washed with phosphate buffer solution for three times. Subsequently, the resultant NPs were dispersed in 4 mL of 10 mmol/L phosphate buffer solution by ultrasonication again, followed by adding 200 μL of 5.0 mg/ml avidin. The mixture was shaken slowly on a shaking table at room temperature for 12 h again. The avidin-conjugated NPs were separated and washed with phosphate buffer solution for three times with the supernatant discarded each time. After final removal of the supernatant, the precipitates dried at 37 °C for 12 h.

5. Characterization of UCNPs and MNPs

In Yb^{3+} and Er^{3+} co-doped systems, Yb^{3+} ions act as sensitizers and Er^{3+} ions as activators. In Figure 2(a), four groups of emission lines appear, peaking at 410, 525, 544, and 655 nm in turn, which are assigned to the $^2H_{9/2}$-$^4I_{15/2}$ (blue), $^2H_{11/2}$-$^4I_{15/2}$ (green), $^4S_{3/2}$-$^4I_{15/2}$ (green), and $^4F_{9/2}$-$^4I_{15/2}$ (red) transitions of Er^{3+} ions, respectively. In Yb^{3+} and Tm^{3+} co-doped systems, Yb^{3+} ions act as sensitizers and Tm^{3+} ions as activators. In Figure 2(b), three groups of emission lines appear, peaking at 362, 452 and 477 nm in turn, which are assigned to the $^1D_2$-$^3H_6$ (ultraviolet), $^1D_2$-$^3F_4$ (blue), $^1G_4$-$^3H_6$ (blue) and $^1G_4$-$^3F_4$ (red) transitions of Tm^{3+} ions, respectively.[5] The inset of Fig.S1a shows a photograph of naked-eye visible red upconversion luminescence of the $NaYF_4$: Yb, Er nanoparticles excited with a commercially available 980 nm laser. The other photograph inset of Fig.S2b shows naked-eye visible blue upconversion luminescence of the $NaYF_4$: Yb, Tm nanoparticles.

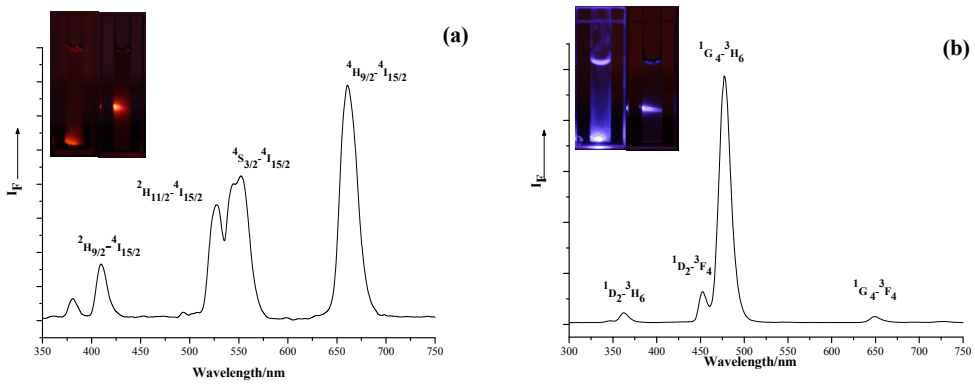

Fig.S1 $NaYF_4$:Yb, Er upconversion luminescence fluorescence spectrum (a), photograph of nanoparticles in a transparent aqueous colloid solution (inset in (a)), and $NaYF_4$:Yb, Tm upconversion luminescence fluorescence spectrum (b), photograph (inset in (b)) excited with a commercially available 980 nm laser.

Typical TEM image of the bare UCNPs synthesized before silica coating is shown in Fig.S2(a,c), the UCNPs are well-dispersed and uniform in size with an average diameter of about 50 nm. It should be noted that the UCNPs synthesized even under relatively stringent conditions (for example, reacted at 195 °C for 18 h) present a regular spherical shape, which is beneficial to their further application in biomolecule. After surface modification by SiO_2, the size of the UCNPs was increased due to the formation of a silica layer on the surface of the bare UCNPs in Fig.S2(b,d).

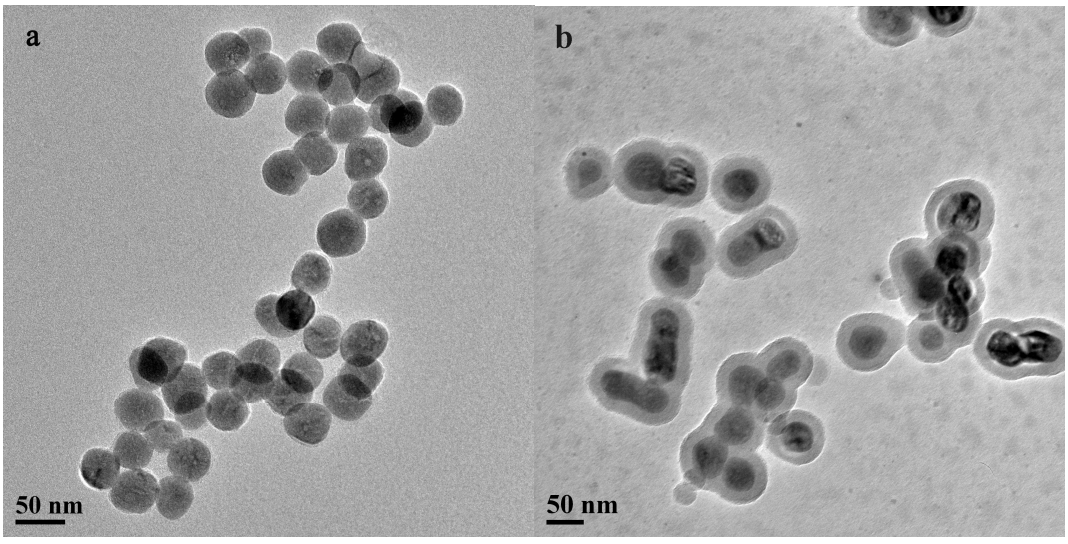

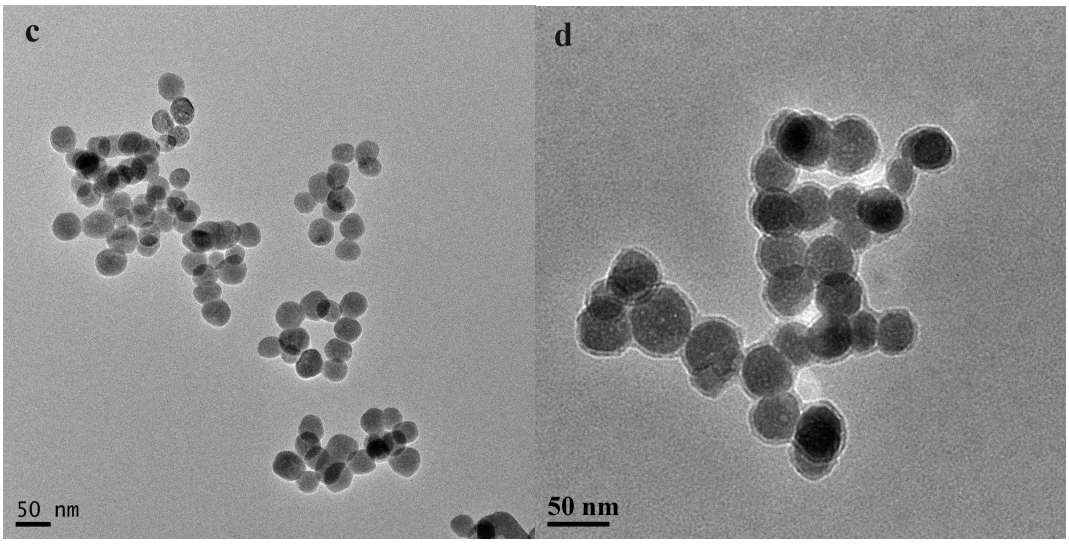

Fig.S2 TEM images of hexagonal phase $NaY_{0.28}F_4$: $Yb_{0.70}$, $Er_{0.02}$ UCNPs synthesized at 195 °C for 18 h (a), TEM images of surface modification of $NaY_{0.28}F_4$: $Yb_{0.70}$, $Er_{0.02}$ UCNPs, the layer of silica-coated was about 10 nm (b), TEM images of hexagonal phase $NaY_{0.78}F_4$: $Yb_{0.20}$, $Tm_{0.02}$ UCNPs (c), the thin layer of silica-coated was about 2 nm (d).

$NaREF_4$ upconversion nanoparticles exist either in cubic α-phase (metastable low -temperature phase) or hexagonal β-phase (thermodynamically stable high -temperature phase) at ambient pressure.[6] In most cases, cubic α-phase $NaREF_4$ can be obtained under mild conditions, such as short reaction time and low temperature. However, hexagonal β-phase $NaREF_4$ can be obtained from α-$NaREF_4$ via a cubic-to-hexagonal phase transition process under relatively drastic conditions, such as long reaction time and high temperature. During the experiment, we found that the reaction time and temperature were two main influential factors in the phase transition of $NaREF_4$ UPNPs. When the reaction time was maintained at 120°C for 6 h, the XRD pattern (Fig.S3a) matched well with that of cubic α-phase $NaYbF_4$ (JCPDS no.77-2042). With the reaction temperature risen to 195 °C and time increased to 12 h, some new diffraction peaks that can be indexed to the hexagonal β-phase $NaYbF_4$ (JCPDS no. 16-0334) are observed (Fig.S3b), the above phenomena can be attributed to the cubic-to-hexagonal phase transition process. When the reaction time is further, the peaks belonging to the hexagonal β-phase are all significantly enhanced, whereas those corresponding to the cubic α-phase are weakened. However, the UCNPs cannot be transformed from cubic α-phase to hexagonal β-phase

completely with a reaction time of 18 h at 195 °C (Fig.S3c).

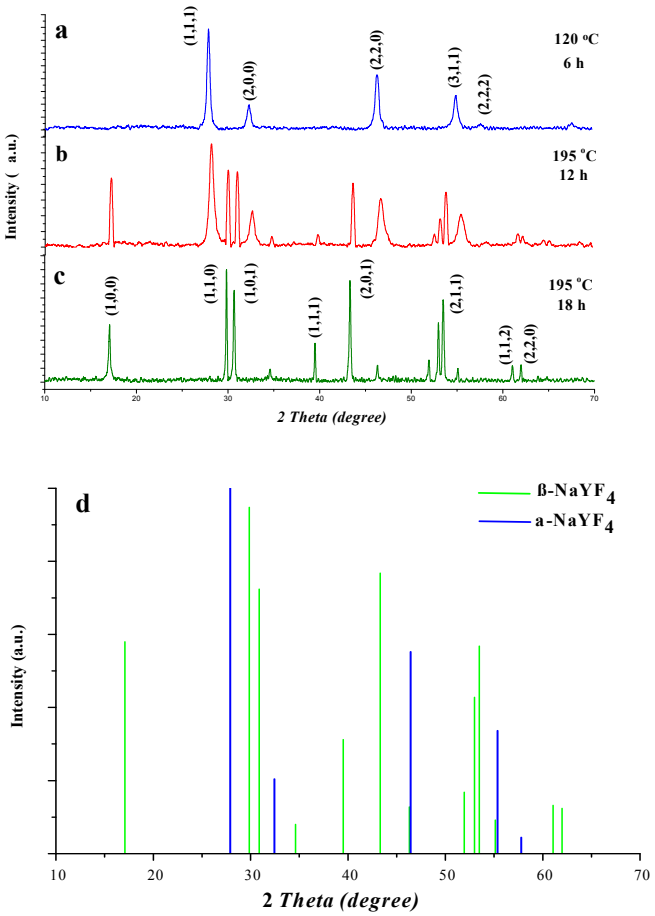

Fig.S3 XRD patterns of $NaY_{0.78}F_4$:$Yb_{0.2}$, $Tm_{0.02}$ UCNPs synthesized at various reaction times and temperatures, at 6 h for 120°C (a), at 12 h for 195°C (b), at 18 h for 195°C (c) as well as the calculated line pattern for cubic α-phase $NaYbF_4$ and hexagonal β-phase $NaYbF_4$ (d).

The functional groups on the surfaces of the amino-modified $NaYF_4$: Yb, Er/Tm UCNPs were identified by FT-IR spectra in Fig.S4. No transmission band appeared with pure hydrothermal-prepared upconversion nanoparticles (Fig.S4). A strong transmission band in the region around 1101 cm^{-1} can be attributed to the symmetrical stretching vibration of the Si-O bond, suggesting that the UCNPs are coated with a layer of silica. The stretching and bending vibration bands of the amine group appear at 3412 and 1629 cm^{-1}, respectively, in the spectrum. In addition, the two peaks at 2925 and 2857 cm^{-1} are corresponding to the asymmetric and symmetric stretching vibrations of the methylene group, respectively, which exists in the hydrolysate of APTES. The peaks at 3412, 2925, and 2857 cm^{-1} together verify the silica-coated UCNPs have been successfully

functionalized with amino groups.

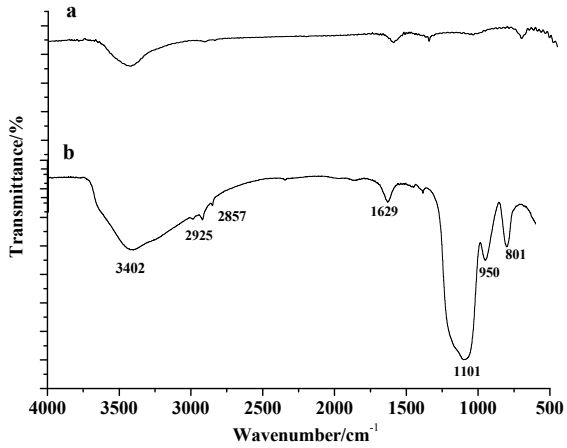

Fig.S4 FT-IR spectrum of the pure upconversion nanoparticles (a) and amino-modified upconversion nanoparticles (b).

The amine-functionalized magnetic nanoparticles applied here were prepared with one-pot synthesis. TEM (Fig.S5a), FT-IR (Fig.S5b) and XRD (Fig.S5c) were demonstrated to characterize the as-synthesized magnetic nanoparticles. From Fig.S5a, it can be seen that the magnetic nanoparticles have an average size of about 25 nm. In addition, these magnetic nanoparticles have good dispersibility and morphology. To provide direct proof for the amine-functionalization, FT-IR spectroscopy was also used to characterize the amine-functionalized magnetite nanoparticles. The strong IR band at 583 cm^{-1} is characteristic of the Fe-O vibrations, while the transmissions around 1400, 1054, and 833 cm^{-1} in Fig.S5b from the amine-functionalized nanocrystals matched well with that from free 1,6-hexadiamine, indicating the existence of the free -NH_2 group on the amine-functionalized nanomaterials. Meanwhile, the XRD (Fig.S5c) results can be easily indexed to Fe_3O_4 (JCPDS 82-1533).

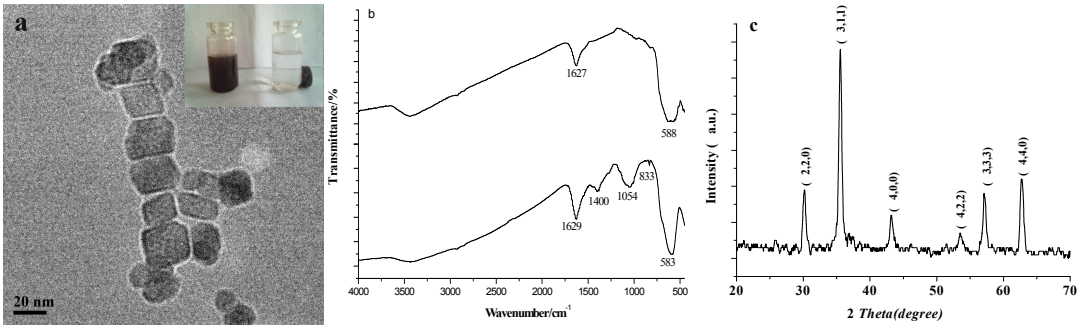

Fig.S5 Characterization of the amine-functionalized magnetic nanoparticles, TEM (a), FT-IR (b),

XRD (c).

6. Characterization of avidin-conjugated nanoparticles

Characterize the combination of nanoparticles with avidin by using a UV-2300 UV-vis spectrophotometer. The results were shown in Fig.S6, we can see that the strong absorbance of avidin at 280 nm. After amine-functionalized nanoparticles and avidin incubated, the supernatant was collected through magnetic separation and centrifugation. The absorbance of the supernatant was observed to be weaker than that of the preliminary avidin solution at 280 nm. The decrease in absorbance is mainly due to the complexing of avidin with amine-functionalized nanoparticles, while the result also verified the nanoparticles have been successfully functionalized with amino groups.

The FI-IR spectrum was more dependably and commonly used to character the functional group. It was also used to comfirm the avidin absorbed on the NPs in our experiment. In comparison with the FT-IR spectrum of the nanoparticles (Fig.S7, curve a,c), the FT-IR spectrum of the resulting displayed obvious absorption peaks corresponding to the amide bands I 1647 cm^{-1} and II 1530 cm^{-1} of avidin appeared (Fig.S7, curve b,d). It demonstrated that the avidin molecules were successfully conjugated to the surface of the NPs.[7]

And the TEM images of avidin-conjugated upconversion nanoparticles (Fig.S8a,b) and magnetic nanoparticle (Fig.S8c) also provided direct proof for water-dispersibility after the avidin molecules on the surface of nanomaterials.

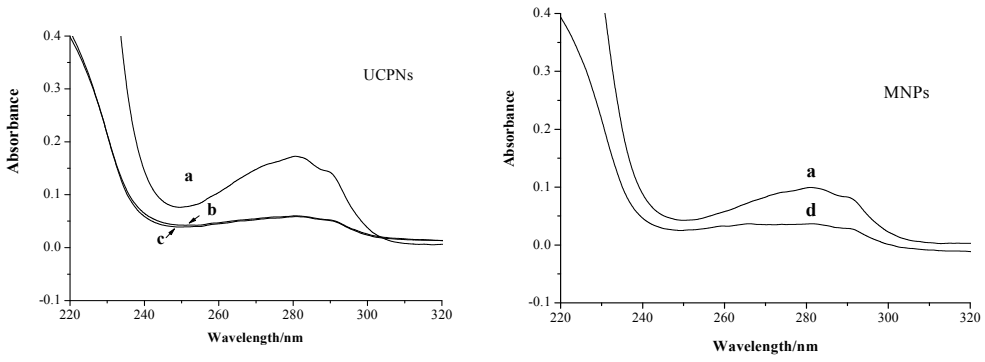

Fig.S6 Absorption spectra of initial avidin solution (a) and supernatant liquor after avidin conjugated amino-modified $NaYF_4$: Yb, Er UCNPs (b), supernatant liquor after avidin conjugated amino-modified $NaYF_4$: Yb, Tm UCNPs (c), supernatant liquor after avidin conjugated amino-modified magnetic nanoparticles (d).

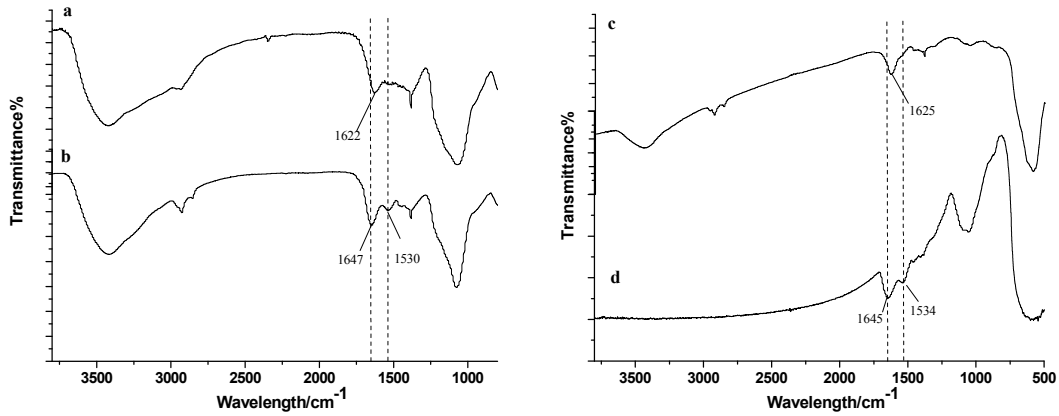

Fig.S7 FT-IR spectrum of amine-functionalized $NaYF_4$@SiO_2 UCNPs nanoparticles (a), avidin-conjugated $NaYF_4$@SiO_2 UCNPs nanoparticles (b), amine-functionalized magnetic nanoparticles (c), avidin-conjugated magnetic nanoparticles (d).

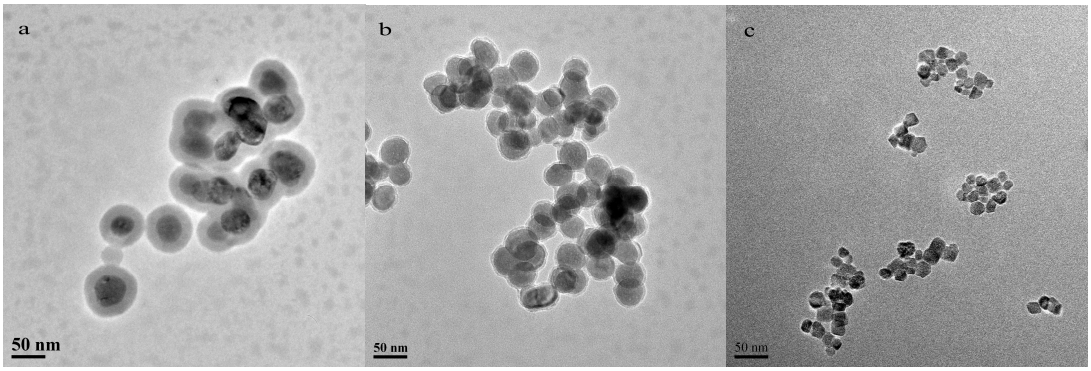

Fig.S8 The TEM images of avidin-conjugated $NaYF_4$: Yb, Er UCNPs (a), avidin-conjugated $NaYF_4$: Yb, Tm UCNPs (b), and avidin-conjugated magnetic nanoparticles (c).

7. The procedure of probe DNA conjugated with UCNPs and the capture DNA conjugate with MNPs

Based upon the hybridization of target DNA strand to luminescent nanoparticle probe with surface immobilized biotin-capped oligonucleotides, two kinds of viral DNA detection schemes have been reported in this work. The $NaYF_4$: Yb, Tm nanoparticles were derivatized with modified DNA1 (EV-71 probe) by incubating ~2 mg/ml of nanoparticle solution overnight with 50 nM of oligonucleotides in 0.1 M PBS (0.1 M NaCl, 10 mM phosphate buffer saline, pH 7.4) at 37 ºC. The $NaYF_4$: Yb, Er nanoparticles were derivatized with modified DNA4 (CV-A16 probe), as well. Following removal of the supernatant, the modified nanoparticles were washed twice with 0.1 M PBS by

centrifugation and redispersion and then finally redispersed in fresh 0.1 M PBS. In the case of magnetic nanoparticles, avidin-conjugated magnetic nanoparticles were prepared adding 250 nM DNA2 and DNA5 (EV-71 capture and CV-A16 capture) to aqueous magnetite nanoparticle solution (particle concentration ~1 mg/ml) in different centrifuge tubes, respectively. The solution was allowed to "age" at 37 ºC for 12 h. Unbound oligonucleotides were subsequently removed by three washing with magnetic separation and still redispersed in fresh 0.1 M PBS.

8. Analytical application

Table 2 Results obtained by the proposed method for EV71 and CV-A16 DNA in diluted PCR products.

Sample	The clinical diagnosis for EV71 by RT-PCR	Concentration of PCR product EV71 by the proposed method (nM)	The clinical diagnosis for CV-A16 by RT-PCR	Concentration of PCR product CV-A16 by the proposed method (nM)
1	+	15.7	+	66.2
2	+	85.7	+	219.9
3	+	35.4	-	ND
4	+	144.6	+	269.8
5	+	102.1	-	ND
6	+	59.6	+	147.3
7	+	62.1	+	119.1
8	-	ND	-	ND

*ND: Not detected

Table 3 Precision and accuracy for the recovery of EV71 and CV-A16 DNA in diluted PCR products.

Analyte	Background content (nM)	Added concentration (nM)	Detected concentration (mean ± SD) (*n*=5),	Recovery ratio %

			(nM)	
EV71	0.857	0.1	0.975±0.15	118.0
		1	1.772±0.23	91.5
		5	5.631±0.38	95.48
CV-A16	0	0.5	0.485±0.17	97.0
		2	2.345±0.47	117.25
		8	7.89±0.63	98.62

1 L. Y. Wang, R. X.Yan, Z. Y. Hao, L. Wang, J. H. Zeng, J. Bao, X. Wang, Q. Peng, Y. D. Li, *Angew. Chem. Int .Ed.,* 2005, **44**, 6054-6057.

2 S. J. Wu, N. Duan, Z. Wang, H. Wang, *Analyst,* 2011,**136**, 2306-2314.

3 W. Stöber and A. Fink, *J. Colloid Interface Sci.,* 1968, **26**, 62-69.

4 L. Y. Wang, J. Bao, L. Wang, F. Zhang, Y. D. Li, *Chem. Eur. J.,* 2006, **12**, 6341-6347.

5 J. F. Suyver, A. Aebischer, D. Biner, P. Gerner, J. Grimm, S. Heer, K.W. Kramer, C. Reinhard, H. U. Güdel, *Opt. Mater.,* 2005, **27**, 1111-1130.

6 H. X. Mai, Y. W. Zhang, R. Si, Z. G. Yan, L. D. Sun, L. P.You, C. H.Yan, *J. Am. Chem. Soc.,* 2006, **128**, 6426-6436.

7 H. F. Dong, F. Yan, H. X. Ji, Y. Wong, H. X. Ju, *Adv. Funct. Mater.,* 2010, **20**, 1173 – 1179.